

# Molecular Clouds as Cosmic-ray Barometers

Sabrina CASANOVA<sup>1</sup>, Felix A. AHARONIAN<sup>1,2</sup>, Yasuo FUKUI<sup>3</sup>, Stefano GABICI<sup>2</sup>, David I. JONES<sup>1</sup>, Akiko KAWAMURA<sup>3</sup>, Toshikazu ONISHI<sup>3</sup>, Gavin ROWELL<sup>4</sup>, Kazafumi TORII<sup>3</sup>, Hiroaki YAMAMOTO<sup>3</sup>

<sup>1</sup>*Max Planck für Kernphysik, Saupfercheckweg 1, 69117, Heidelberg*

<sup>2</sup>*Dublin Institute for Advance Physics, 31 Fitzwilliam Place, Dublin 2, Ireland*

<sup>3</sup>*Nagoya University, Furo-cho, Chikusa-ku, Nagoya City, Aichi Prefecture, Japan*

<sup>4</sup>*School of Chemistry and Physics, University of Adelaide, Adelaide 5005, Australia*

(Received ; accepted )

## Abstract

The advent of high sensitivity, high resolution  $\gamma$ -ray detectors, together with a knowledge of the distribution of the atomic hydrogen and especially of the molecular hydrogen in the Galaxy on sub-degree scales creates a unique opportunity to explore the flux of cosmic rays in the Galaxy. We here present the new data on the distribution of the molecular hydrogen from a large region of the inner Galaxy obtained by the NANTEN Collaboration. We then introduce a methodology which aims to provide a test bed for current and future  $\gamma$ -ray observatories to explore the cosmic ray flux at various positions in our Galaxy. In particular, for a distribution of molecular clouds, as provided by the NANTEN survey, and local cosmic ray density as measured at the Earth, we estimate the expected GeV to TeV  $\gamma$ -ray signal, which can then be compared with observations and use to test the cosmic ray flux.

**Key words:** ISM: clouds, ISM: cosmic rays, ISM: supernova remnants, gamma rays: theory

## 1. Introduction

The question of the distribution of the cosmic rays (CRs) and of the CR sources in the Galaxy was addressed extensively by many authors (see for instance Ginzburg & Syrovatskii 1964 ). Secondary CR data tell us that CR protons and nuclei, that are accelerated by Galactic sources, have a confinement time in the Galaxy of about  $10^7$  years at GeV energies, which decreases with increasing energy. During this time the particles accelerated by individual sources mix together, lose memory of their origin, and contribute to the bulk of Galactic CRs known as the cosmic ray *sea* or CR background.

Direct measurements provide the CR spectrum and flux only in the vicinity of the Solar System and the level of the CR spectrum and flux in other regions of the Galaxy is unknown. In order to investigate the CR level in distant regions of the Galaxy and the distribution of Galactic CR sources one can start assuming that the CR flux and spectrum measured locally is representative of the typical CR flux and spectrum present throughout the Galaxy, except in the proximity of isolated CR sources. The implications of such an assumption are firstly, that there exists a definable CR *sea* of homogenised and isotropised CRs, far from any of the kpc-scale uniformly and continuously distributed CR sources, which is the typical CR flux and spectrum in the Galaxy; and secondly, that the Earth sits in a typical region far from any source where this *sea* can be measured directly. Although the  $10^7$  years diffusion time of CRs in the Galaxy seems to imply the existence of the *sea*, in principle there could indeed be a *sea* of CRs in the Galaxy, but the Earth could be located close to a so far undetected CR source, so that the locally measured flux is

therefore substantially higher than the *sea* and the spectrum substantially harder, and the local values are therefore not representative of the typical case. Alternatively, if the CR sources are distributed quite densely, on sub-kpc scales in the Galaxy, there may not really be a *sea* CR spectrum at all. The local values of CR flux and spectrum would then vary strongly depending mostly on the proximity to the CR sources in any particular region. In this case the flux value at the Earth could be lower or higher, and the spectrum softer or harder, than any given distant region. Finally, it could be that the CR sources are so densely distributed in the Galaxy, that there might exist strong gradients in the CR spectrum, depending mostly on the proximity to the CR sources in any particular region, and the Earth might by chance be located unusually far from any source and thus the locally measured flux and spectrum are lower and softer than typical values found elsewhere.

Whilst diffusing through the Galaxy, CRs interact with ambient matter (both molecular and atomic) and produce  $\gamma$ -rays through inelastic collisions. This emission has long been recognised by many authors as a unique probe of the parent CR distribution because the resultant  $\gamma$ -ray emissivity is a function only of the matter density and the CR spectrum (Ginzburg & Syrovatskii 1964 ; Puget & Stecker 1974 ; Casse & Cesarsky 1976 ; Bloemen et al 1984 ; Bloemen et al 1986 ; Lebrun et al. 1982 ; Bertsch et al. 1993 ; Hunter et al. 1997 ; Strong et al. 2004 ). For instance Bloemen et al 1986 investigated the galacto-centric distribution of cosmic rays. They defined four intervals in the galacto-centric radius, for which they calculated the column densities of atomic and molecular hydrogen. By comparing the  $\gamma$ -ray intensities with the predicted emis-

sivities, they derived an exponential distribution for the cosmic rays in the Galaxy. In the paper by Bertsch et al. 1993 the CR flux used for calculating the  $\gamma$ -ray flux is varied position to position by multiplying by a "cosmic ray enhancement factor"  $c(r, l, b)$ , which is derived by convolving the matter distribution with a Gaussian distribution whose width is an adjustable parameter  $r_0$ . The cosmic ray enhancement factor  $c(r, l, b)$  takes a value ranging from 0.1 to 1.6. The CR flux in the Galaxy varies significantly to that measured in the solar neighbourhood. The most comprehensive numerical model, which includes particle production and propagation in the Galaxy, is GALPROP (Strong et al. 2004)<sup>1</sup>. GALPROP is designed to perform cosmic-ray propagation calculations for nuclei, antiprotons, electrons and positrons, and computes diffuse  $\gamma$ -rays and synchrotron emission. In GALPROP the CR propagation equation is solved numerically on a spatial grid, either in 2D with cylindrical symmetry in the Galaxy or in full 3D. The numerical solution proceeds in time until a steady-state is reached. Normalisation of protons, helium and electrons to experimental data is provided (all other isotopes are determined by the source composition and propagation).  $\gamma$ -rays and synchrotron are computed using interstellar gas data (for pion-decay and bremsstrahlung) and the interstellar radiation fields (ISRF) model (for inverse Compton). Spectra of all species on the chosen grid and the  $\gamma$ -ray and synchrotron sky-maps are output in a standard astronomical format for comparison with data. The approach adopted by Strong et al. 2004 to include effects of CR flux variations in the Galaxy is to calculate the propagation effect from CR sources, which results in variation of CR flux in our Galaxy (Strong & Moskalenko 1998). The simulated  $\gamma$ -ray flux is then the background, which must be subtracted to recognise the sites of concentrated excess  $\gamma$ -ray emission in a detector data, such as in Fermi data.

Interestingly, based on EGRET data (Hunter et al. 1997) the  $\gamma$ -ray emission from the inner Galaxy ( $300^\circ < l < 60^\circ$  and  $-10^\circ < b < 10^\circ$ , as defined in Hunter et al. 1997) at energies greater than about 1 GeV exceeds, by some 60%, the intensity predicted by model calculations Bertsch et al. 1993; Hunter et al. 1997. Recent observations, performed by the LAT instrument on board the Fermi satellite, show that the spectra of the Galactic diffuse emission at MeV-GeV energies, at least at intermediate latitudes (Abdo et al. 2009), can be explained by cosmic-ray propagation models based on local observations of cosmic-ray electron and nuclei spectra. On the other hand, at TeV energies the spectral features of the  $\gamma$ -ray emission detected by HESS from the Galactic centre (GC) region (Aharonian et al. 2006), and the emission measured by Milagro from the Cygnus Region (Abdo et al. 2007; Abdo et al. 2008), suggest that the CR flux might significantly vary in the different locations of the Galaxy.

In this paper we seek to compare the CR flux and spectrum observed at the Earth to the CR flux and spectrum in specific distant regions, derived from observations of

$\gamma$ -rays emitted by CRs propagating through molecular clouds. We first present not publicly available CO observations obtained with the NANTEN telescope for a significant and interesting part of the galactic plane. We then demonstrate that the NANTEN data in combination with the Fermi data allow meaningful studies of deviations of the cosmic ray flux from the average one. The level of the *sea* of lower energy CRs ( $< \text{few GeV}$ ) has been traced by the ionisation rate inferred from different molecular species seen in molecular clouds (Indriolo et al. 2007; Indriolo et al. 2009). The level of the CR *sea* above 1 GeV will then be inferred by combining the  $\gamma$ -ray emission from molecular clouds with the data from the Leiden/Argentine/Bonn (LAB) survey of the Galactic atomic hydrogen (Karberla et al. 2005) and from the NANTEN survey of Galactic molecular hydrogen (Fukui et al 1999; Mizuno & Fukui 2004; Fukui et al. 2001; Fukui et al. 2008). Studying the  $\gamma$ -ray emission from single molecular clouds the differential, local distribution of the cosmic ray flux can be inferred. The detection of even a single under-luminous cloud with respect to the predictions based on the local CR density would cast severe doubt on the assumption that the level of the observed CR flux is representative of the average CR flux and spectrum in the Galaxy.

In Section 2 we will present new data on the distribution of the molecular hydrogen from the region of the inner Galaxy, which spans Galactic longitude  $340^\circ < l < 350^\circ$  and Galactic latitude  $-5^\circ < b < 5^\circ$ , obtained by the NANTEN Collaboration. We will also briefly review the results of the LAB survey of the Galactic atomic hydrogen. A description of our approach will be given in Section 3. The method will be here applied to the region of the Galactic Plane described above to provide a 'proof-of-concept'. A more comprehensive study on a larger scale will be discussed in a future paper. Some predictions concerning the  $\gamma$ -ray and cosmic ray fluxes from molecular clouds including their uncertainties are given in Section 4, where we will also discuss the observational prospects for present and future observatories. Our conclusions are given in Section 5.

## 2. The gas distribution

### 2.1. The NANTEN survey of molecular hydrogen

The NANTEN instrument is a 4 m millimetre/sub-millimetre telescope which has surveyed the southern sky using the  $^{12}\text{CO}$  (J=1-0) emission line at 115.271 GHz ( $\lambda = 2.6$  mm). The angular resolution at this frequency is  $4'$ , with a mass sensitivity of about  $100 M_\odot$  at the Galactic centre (GC), assuming a distance of 8.5 kpc for the GC. The NANTEN data set has 1 km/s resolution in velocity (Mizuno & Fukui 2004; Fukui et al 1999; Fukui et al. 2001; Fukui et al. 2008). The conversion factor,  $X$ , which is used to translate the intensity of CO molecular line emission into  $\text{H}_2$  column density (Nakanishi & Sofue 2003; Nakanishi & Sofue 2006), is assumed to be

$$X = 1.4 \times 10^{20} e^{(R/11 \text{ kpc})} [\text{cm}^{-2} \text{K}^{-1} \text{km}^{-1} \text{s}], \quad (1)$$

<sup>1</sup> GALPROP is available from: <http://galprop.stanford.edu/>

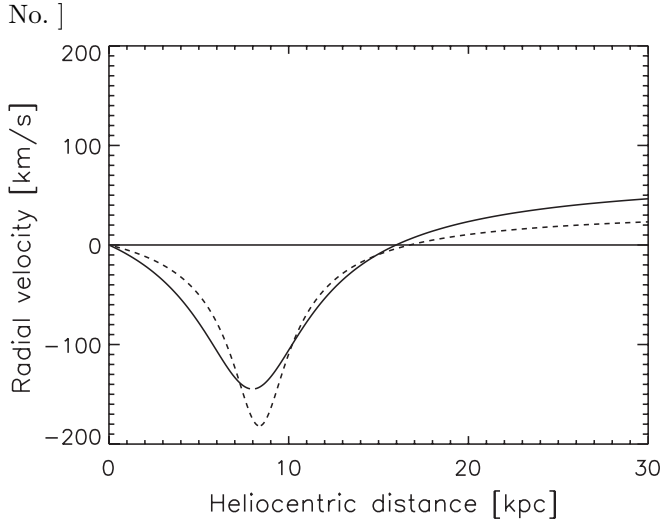


**Fig. 1.** The radial velocity vs heliocentric distance estimated from flat rotation of the galactic disk is shown. The solid line is at  $(l,b)$  (340,0) and the dashed line is at  $(l,b)$  (350,0).

where  $R$  is distance to the GC. This conversion factor, which is based on the metallicity distribution in the Galaxy, is a function of the distance to the GC. The uncertainty in the determination of the distance to the GC and in the determination of the calibration itself leads to an uncertainty in  $X$  of a factor of 50% (Arimoto et al. 1996).

The final data product for the region, which spans Galactic longitude  $340^\circ < l < 350^\circ$  and Galactic latitude  $-5^\circ < b < 5^\circ$ , consists of a  $150 \times 150 \times 600$  element three-dimensional image of the molecular hydrogen distribution as a function of Galactic longitude, latitude and velocity. Assuming a flat rotation curve model of the Galaxy with uniform velocity equal to 220 km/s, the data-cubes in longitude, latitude and velocity are transformed to data-cubes in longitude, latitude and heliocentric distance (Nakanishi & Sofue 2003 ; Nakanishi & Sofue 2006 ).

Figure 1 shows a plot of the radial velocity versus heliocentric distance used to convert the velocity information into distance. There are two distance solutions for each radial velocity in the inner Galaxy. In order to resolve this near-far distance ambiguity, the method by (Nakanishi & Sofue 2003 ; Nakanishi & Sofue 2006 ) is used. The principle uncertainty in the determination of the distances in the NANTEN data-set comes from errors in the accuracy of the radial velocity estimates. The combination of turbulence and peculiar proper motions of the gas causes spectral line broadening, which introduces uncertainties in the radial velocity, that can be as large as 15 km/s (a giant molecular cloud typically shows velocity width of 10 km/s, and the cloud-cloud motion is 3-3.9 km/s (Alvarez et al. 1990 ; Clemens 1985 )). This corresponds to an uncertainty of less than 2 kpc in the distance. The dependence of the uncertainties in the radial velocity on the particular location is small for our dataset, since the longitude range used here includes disk gas, and excludes the Galactic centre and molecular ring. For disk gas, it is, in fact, unlikely to have significant systematic variation in either cloud-cloud velocity dispersion or typical line widths

with location. Correspondingly, the distance error arising from molecular gas velocity dispersion is likely to be fairly constant throughout our data sample.

### 2.1.1. Gas morphology

Figure 2 (Left) and 2 (Right) show NANTEN observations of the  $^{12}\text{CO}$  ( $J=1-0$ ) emission line from a large area of the Galactic plane. This segment spans Galactic longitude  $340^\circ < l < 350^\circ$  and Galactic latitude  $-5^\circ < b < 5^\circ$ . Figure 2 (Left) shows the integrated emissivity in units of  $\text{cm}^{-3} \text{ km s}^{-1}$  from this region. Inspection of Figure 2 (Left) shows that the molecular material is predominantly confined to  $\lesssim 2^\circ$  of the plane. The longitude span places this region in between the Galactic centre and the Norma arm (Duncan et al. 1995 ) so that there should be no contamination from depth effects from looking down an arm. This is reflected in the distribution of heliocentric distance in the region in Figure 2 (Right), which shows the distance as a function of position. Figure 2 (Right) shows, in fact, a moment 1 map of the region, which is  $\sum[I d] / \sum[I]$ , where  $I$  is the intensity and  $d$  is the distance of the gas and has units of kilo-parsec. There are a few regions of emission which are very far away (corresponding to the dark pixels). However, these tend to be isolated, small segments on the edge of the plane, and hence they should contribute a negligible amount to the  $\gamma$ -ray emissivity. Specifically, Figure 2 (Right) shows that the bulk of the observed emission originates at distances of  $\lesssim 2$  kpc, whilst there is some emission, mainly confined to the central regions of the Galactic plane, which are at greater distances.

### 2.2. The Leiden/Argentine/Bonn Galactic HI Survey

We use data from the Leiden/Argentine/Bonn (LAB) Galactic HI Survey <sup>2</sup> (Karberla et al. 2005 ) for the distribution of the atomic hydrogen. The LAB observations were centred on the 1420 MHz ( $\lambda 21$  cm) line with a bandwidth of 5 MHz. The velocity axis spans  $-450 \text{ km s}^{-1}$  to  $400 \text{ km s}^{-1}$  giving a final velocity resolution of  $1.3 \text{ km s}^{-1}$ . The data combines observations from three telescopes at a common resolution of  $0.6^\circ$  with a final sensitivity of  $\sim 0.1$  K. We used the same procedure described in 2.1 to transform the velocity axis into distance.

### 3. Testing the level of the CR background

The emissivity of molecular clouds located far away from CR sources, so called *passive* molecular clouds, i.e. clouds which are illuminated by the supposedly existing CR background, can be used to probe the level of the CR *sea* (Issa and Wolfendale 1981 ). Given that the  $\gamma$ -ray -emission from the molecular cloud depends only upon the total mass of the cloud,  $M$ , and its distance from the Earth,  $d$ , the CR flux,  $\Phi_{CR}$ , in the cloud is uniquely determined as

$$\Phi_{CR} \propto \frac{F_\gamma d^2}{M} \quad (2)$$

<sup>2</sup> available from:  
[http://www.astro.uni-bonn.de/~webaiub/english/tools\\_labsurvey.php](http://www.astro.uni-bonn.de/~webaiub/english/tools_labsurvey.php)

where  $F_\gamma$  is the integral  $\gamma$ -ray flux from the cloud and  $M = nV$ , with  $n$  the gas number density and  $V$  the volume of the cloud. Under the assumption that the CR background is equal to the locally observed CR flux, the calculated  $\gamma$ -ray flux from the cloud can be compared to the observed  $\gamma$ -ray flux in order to probe the CR spectrum in distant regions of the Galaxy. The detection of under-luminous clouds with the respect to predictions based on the CR flux at Earth would suggest that the local CR density is enhanced with respect to the Galactic average density. This would cast doubts on the assumption that the local CRs are produced only by distant sources, and that the CR flux and spectrum measured locally is representative of the typical CR flux and spectrum present throughout the Galaxy (Aharonian 2001).

### 3.1. Diffusion of CRs into molecular clouds

The diffusion of CRs into molecular clouds depends upon the highly uncertain diffusion coefficient. CRs can penetrate clouds if the diffusion coefficient inside the molecular clouds is the same as the average diffusion coefficient in the Galaxy, as derived from spallation measurements. CRs are effectively excluded if the diffusion coefficient is suppressed (Gabici, Aharonian & Blasi 2007). However, it has been shown that CRs at TeV energies can diffuse into even the densest parts of molecular clouds. Whilst GeV energy CRs can diffuse into typical Galactic molecular clouds (Gabici et al. 2009), they have trouble penetrating the densest parts of particular molecular clouds, such as the GC giant molecular cloud, Sagittarius B2 ((Jones et al. 2009) and references therein).

### 3.2. Computational procedure

Under the assumption that the CR background in the region of longitude range  $340^\circ < l < 350^\circ$  and latitude range  $-5^\circ < b < 5^\circ$  is uniform and equal to the locally observed CR flux we calculate the spectral features and the longitudinal and latitudinal profiles of the  $\gamma$ -ray emission. We will then proceed to infer the missing information concerning the distance from the Sun to complete the 3D view of the  $\gamma$ -ray emission.

#### 3.2.1. Spectral feature of the emission

The differential photon flux at Earth produced by CRs interacting with the gas from a given region in the Galaxy is

$$\frac{dN_\gamma}{dAdE_\gamma dt d\Omega} = \int dl_d \int \frac{d\sigma_{p \rightarrow \gamma}}{dE_p} n(l, b, l_d) J(E_p) dE_p \quad (3)$$

where the integrals are over the heliocentric distance,  $l_d$  and over the energy of the protons,  $E_p$ .  $n(l, b, l_d)$  is the gas density as function of the heliocentric coordinates, latitude,  $b$ , longitude,  $l$ , and  $l_d$ , and  $J(E_p)$  is the proton spectrum. In Equation (3) the spectral dependence of the photons emitted by CR protons, expressed in terms of the differential cross section,  $d\sigma_{p \rightarrow \gamma}/dE_p$ , is calculated using the parametrisation of Kelner et al. 2006. A multiplication factor of 1.5, applied to the proton spectrum, accounts for the contribution to the emission from heavier

nuclei both in CRs and in the interstellar medium (Dermer 1986; Mori 1997). From Equation (3) for a uniform distribution of CRs the  $\gamma$ -ray spectrum is given as

$$\frac{dN_\gamma}{dAdE_\gamma dt d\Omega} = \int dE_p \frac{d\sigma_{p \rightarrow \gamma}}{dE_p} J(E_p) \int dl_d n(l, b, l_d), \quad (4)$$

where the integral over the line of sight,  $l_d$ , defines the gas column density for a given direction in latitude and longitude. The average atomic and molecular hydrogen column densities for the region of the Galaxy of longitude range  $340^\circ < l < 350^\circ$  and latitude range  $-5^\circ < b < 5^\circ$  are  $3.3 \times 10^{21} \text{ cm}^{-2}$  and  $1.4 \times 10^{22} \text{ cm}^{-2}$ , respectively. The CR spectrum is assumed to be equal to the CR flux measured at the top of the Earth's atmosphere. Below  $10^6$  GeV we here adopt the value of

$$J(E_p) = 1.8 E_p^{-2.7} \text{ cm}^{-2} \text{ s}^{-1} \text{ sr}^{-1} \text{ GeV}^{-1}, \quad (5)$$

taken from the Particle Data Group 2008. A change in the spectral index of the measured CR flux is observed above  $10^6$  GeV, which we do not consider as we are interested in the  $\gamma$ -ray emission below 100 TeV.

#### 3.2.2. Longitudinal and latitudinal profiles of the emission

The latitudinal and longitudinal profiles of the  $\gamma$ -ray emission due to protons scattering off the atomic and molecular hydrogen from the region which spans Galactic longitude  $340^\circ < l < 350^\circ$  and Galactic latitude  $-5^\circ < b < 5^\circ$  are shown in Figure 3 (*Left*) and (*Right*) respectively. The  $\gamma$ -ray profiles which the Fermi telescope would observe are plotted for 1 GeV and 10 GeV. For a Cherenkov telescope, such as CTA, we show the  $\gamma$ -ray profiles at 100 GeV and 1 TeV. The instrument point spread functions at the different energies are also taken into account.

A peak in the emission at longitude of about  $345.7^\circ$  close to the Galactic Plane is clearly visible, next to a dip in the longitude profile. While the atomic gas is generally broadly distributed along the Galactic Plane, the molecular hydrogen is less uniformly distributed and the peaks in the  $\gamma$ -ray longitude profiles correspond to the locations of highest molecular gas column density. The peaks in the longitudinal profile reveal the directions in the Galaxy where massive clouds associated with spiral arms are aligned along the line of sight. In the following discussion we will further analyse the region of latitude range  $1^\circ < b < 1.7^\circ$  and longitude range  $345.3^\circ < l < 346^\circ$ , where the peak in the  $\gamma$ -ray profiles is located.

#### 3.2.3. Localisation of the emission along the line of sight distance

In order to localise the region along the line of sight,  $l_d$ , where most  $\gamma$ -rays are emitted, Figures 4 and 5 (*Middle*) show the atomic and molecular hydrogen densities as a function of the line of sight distance, averaged over the inner  $1^\circ < b < 1.7^\circ$  of the Galactic plane in the region of longitudes  $345.3^\circ < l < 346^\circ$ . The value of the gas density is given every 50 pc from 50 pc up to 30 kpc from the Sun. The density of the atomic hydrogen as function of the heliocentric distance,  $l_d$ , shown in Figure 4 (*Middle*), tends to be quite uniform. On the other hand, the plot

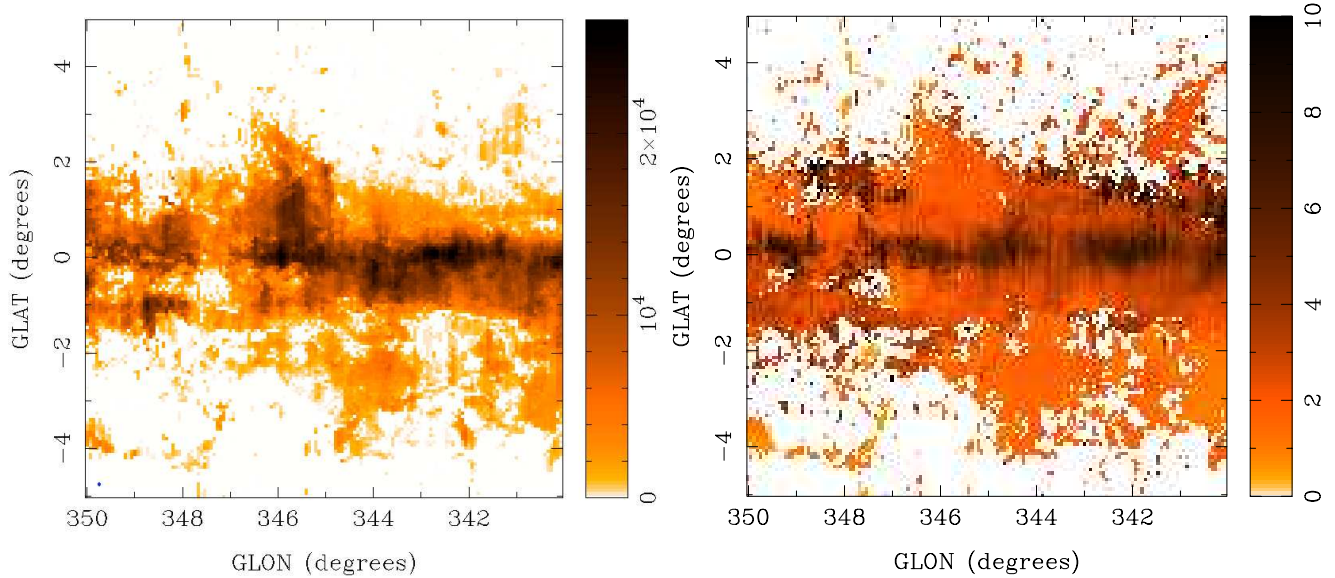


**Fig. 2.** (Left): Integrated intensity image for the CO ( $J=1-0$ ) line emission obtained by the NANTEN telescope for the region  $340^\circ < l < 350^\circ$  and  $-5^\circ < b < 5^\circ$ . The intensity scale on the right is in units of  $\text{km s}^{-1} \text{cm}^{-3}$  with the  $4'$  beam located in the lower left-hand corner. (Right): Position-distance image (i.e., moment 1) of the region of interest. The intensity scale on the right is in units of kpc. A logarithmic scaling has been applied to both images to emphasise the low-level emission.

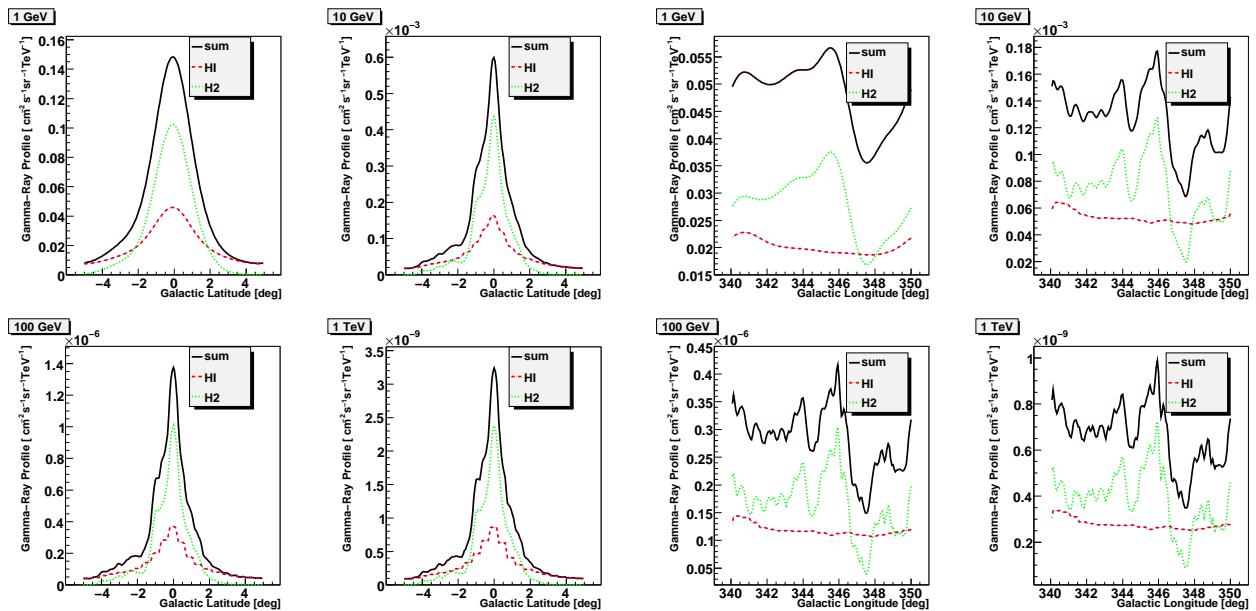


**Fig. 3.** (Left 4 panels) The latitudinal profile of the  $\gamma$ -ray emission due to CRs scattering off atomic and molecular hydrogen at different energies which would be measured by Fermi and a Cherenkov telescope such as CTA from the region  $-5^\circ < b < 5^\circ$ , integrated over the longitude range  $340^\circ < l < 350^\circ$ . The emission is convolved with the energy dependent PSF of Fermi at 1 GeV and 10 GeV, and of a future Cherenkov telescope at 100 GeV and 1 TeV. The energy dependence of the Fermi PSF can be found at: <http://www-glast.slac.stanford.edu/software/IS/glastlatperformance.htm>. We adopt a point spread function of  $0.05^\circ$  at 100 GeV and  $0.02^\circ$  at 1 TeV. The dotted green lines are for the emission arising from CRs scattering off molecular hydrogen, the dashed red ones for the emission arising from CRs scattering off atomic hydrogen and the solid black ones for the sum. The  $\gamma$ -ray profile is in units of  $\text{cm}^{-2} \text{s}^{-1} \text{sr}^{-1} \text{TeV}^{-1}$ . (Right 4 panels) The longitudinal profile of the  $\gamma$ -ray emission from the region  $340^\circ < l < 350^\circ$ , integrated over the latitude range  $-5^\circ < b < 5^\circ$ . The emission is convolved with the energy dependent PSF of Fermi at 1 GeV and 10 GeV, and of a future Cherenkov telescope such as CTA at 100 GeV and 1 TeV. The dotted green lines are for the emission arising from CRs scattering off molecular hydrogen, the dashed red ones for the emission arising from CRs scattering off atomic hydrogen and the solid black ones for the sum. The  $\gamma$ -ray profile is in units of  $\text{cm}^{-2} \text{s}^{-1} \text{sr}^{-1} \text{TeV}^{-1}$ .

in Figure 5 (*Middle*) shows that much of the molecular material is located within  $\lesssim 2 - 3$  kpc, which reinforces the evidence presented in Figure 2 (*Right*). As Figure 5 (*Middle*) shows, the molecular hydrogen density peaks to  $n_{\text{H}_2} = 20 \text{ cm}^{-3}$  in this region.

The total mass ( $\text{H}_2$  and HI) in the element of volume,  $\Delta V = l_d^2 \cos(b) \Delta b \Delta l \Delta l_d$ , with  $\Delta b = \Delta l = 0.01 \text{ rad}$  ( $= 0.7^\circ$ ) and  $\Delta l_d = 50 \text{ pc}$  around the directions of longitude  $345.7^\circ$  and latitude  $1.3^\circ$ , is

$$\Delta M = n(l, b, l_d) \Delta V. \quad (6)$$

$\Delta M$  is calculated every 50 parsecs along the line of the sight distance,  $l_d$ , corresponding to each value of the gas density  $n(l, b, l_d)$ . In Figures 4 and 5 (*Top*) we plot the mass per unit distance  $\Delta M / \Delta l_d$  in a volume element in units of  $M_5 \text{ kpc}^{-1}$  where  $M_5 = 10^5 M_\odot$ .

Assuming the local CR flux, the unit volume emissivity above a given energy,  $E^*$ , is proportional to the total mass in the element of volume,  $\Delta V$ , and in photons  $\text{cm}^{-2} \text{ s}^{-1} \text{ kpc}^{-1}$  it is

$$\begin{aligned} \Delta F(E > E^*) &= 1.2 \times 10^{-13} \left( \frac{E^*}{1 \text{ TeV}} \right)^{-1.7} \\ &\times \left( \frac{l_d}{1 \text{ kpc}} \right)^{-2} \frac{\Delta M}{M_5}. \end{aligned} \quad (7)$$

The emissivity per unit volume as a function of the line of sight distance,  $\Delta F(E > E^*) / \Delta l_d$ , is plotted in Figures 4 and 5 (*Bottom*). Figures 4 and 5 (*Bottom*) show that most of the  $\gamma$ -ray emission from the region of longitude  $345.3^\circ < l < 346^\circ$  and latitude  $1^\circ < b < 1.7^\circ$  is produced between 0.5 and 3 kpc.

The combined longitudinal, latitudinal and distance profiles provide together a tomographical view of the  $\gamma$ -ray emission. The investigation of the distribution of the  $\gamma$ -ray emission gives the locations in the Galaxy where most  $\gamma$ -ray emission is produced within a reasonably limited region, where a single or at most few massive clouds are located, making it possible to constrain the CR flux in this particular region.

### 3.3. Leptonic emission and secondary electrons

#### 3.3.1. Leptonic Emission: The Inverse Compton and Bremsstrahlung Contribution

Inverse Compton scattering of cosmic ray electrons results in a non-negligible contribution to the overall diffuse  $\gamma$ -ray emission at GeV, and perhaps also at TeV energies (see e.g. (Aharonian & Atoyan 2000)). However the relative contribution of this component (compared to the bremsstrahlung and  $\pi^0$ -decay  $\gamma$ -rays) from specific dense regions is significantly reduced because of the enhanced gas density. The ratio of the bremsstrahlung-to  $\pi^0$ -decay  $\gamma$  rays does not depend on the density. However, the contribution of the bremsstrahlung to the total diffuse emission above 1 GeV is rather low, so it can be ignored. This is true also for the bremsstrahlung from secondary electrons. Therefore in this paper we will focus only on the  $\pi^0$ -decay component.

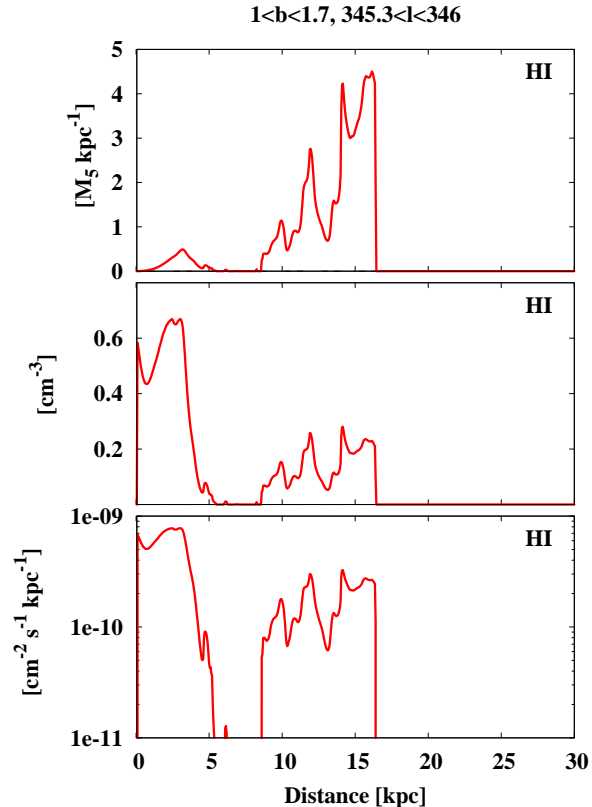


**Fig. 4.** (*Top*): Total HI mass per unit distance ( $(\Delta M / \Delta d)$ ) in a volume element in  $10^5 M_\odot \text{ kpc}^{-1}$  from the direction  $345.7^\circ$  in Galactic longitude and  $1.3^\circ$  in Galactic latitude is shown. (*Middle*): Gas density as a function of heliocentric distance  $l_d$ . (*Bottom*): Unit volume emissivity above 1 GeV as a function of  $l_d$  in units of  $\text{cm}^{-2} \text{ s}^{-1} \text{ kpc}^{-1}$ .

#### 3.3.2. Possible Role of Secondary Electrons and Positrons

When CRs interact with ambient matter through inelastic collisions they produce not only neutral pions, but also charged pions. These charged pions emit secondary electrons, positrons and neutrinos. Thus, in addition to the  $\gamma$ -ray emissivity due to neutral pion decay, there will be a simultaneous radio synchrotron component due to the secondary electrons and positrons produced concomitantly with the neutral pions. Whilst the emissivity of such electrons is beyond the scope of this paper, we pause only to note that their emissivity is proportional to the mass of ambient matter and the CR flux in most regions. In the densest regions (i.e.  $> 10^4 \text{ cm}^{-3}$ ) however, the synchrotron emissivity will scale as the volume because of the increased efficiency of bremsstrahlung cooling (Jones et al. 2009). Since synchrotron emission from secondaries is not readily observable in the cases so far attempted (Jones et al. 2008; Protheroe et al. 2008), this method of checking the validity of the CR-sea assumptions at GeV energies is probably not feasible.

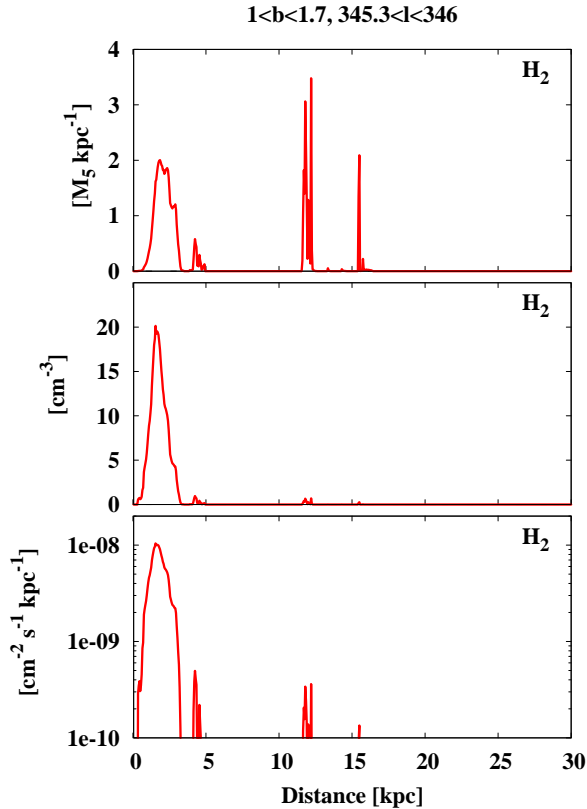


**Fig. 5.** (Top): Total  $H_2$  mass per unit distance ( $(\Delta M/\Delta d)$ ) in a volume element in  $10^5 M_\odot \text{ kpc}^{-1}$  from the direction  $345.7^\circ$  in Galactic longitude and  $1.3^\circ$  in Galactic latitude is shown. (Middle): Gas density as a function of distance  $d$ . (Bottom): Flux above 1 GeV in units of  $\text{cm}^{-2} \text{ s}^{-1} \text{ kpc}^{-1}$ .

#### 4. Results and Discussion

Table 1 shows the total hydrogen mass from the LAB and NANTEN surveys and the integral  $\gamma$ -ray flux above 1 GeV and above 100 GeV as a function of the line of sight,  $l_d$ , from the region  $345.3 < l < 346^\circ$  and  $1^\circ < b < 1.7^\circ$  centred on  $l = 345.7^\circ$  and  $b = 1.3^\circ$ . The values for the masses and fluxes are obtained by integrating Equation (6) and (7), respectively, along given portions of the distance,  $l_d$ . It is instructive to note that 2% of the emission comes from the region  $d < 0.5 \text{ kpc}$ , 85% from the region  $0.5 \text{ kpc} < d < 3 \text{ kpc}$ , and 13% from the region  $d > 3 \text{ kpc}$ . The peak in the  $\gamma$ -ray emission in Figure 3 from the direction  $345.7^\circ$  close to the Galactic plane is mostly produced within 0.5 kpc and 3 kpc distance from the Sun. Thus the  $\gamma$ -ray emission from this direction provides a unique probe of the CR spectrum in 0.5-3 kpc, provided the  $\gamma$  emission morphology is shown to match the gas in this distance range. In Figure 6 we show the predicted  $\gamma$ -ray spectra for the same region,  $345.3^\circ < l < 346^\circ$  and  $1^\circ < b < 1.7^\circ$ , arising from the CR spectrum in Equation (5). As shown in Figure 7, the contribution to the emission from the atomic hydrogen in the  $0.5 \text{ kpc} < d < 3 \text{ kpc}$  amounts to about 10%

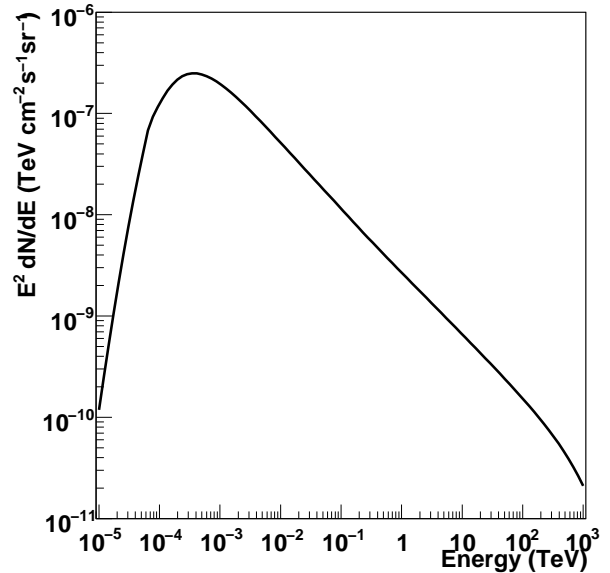


**Fig. 6.** The spectra of the  $\gamma$ -ray emission from the region  $345.3^\circ < l < 346^\circ$  and  $1^\circ < b < 1.7^\circ$  arising from the observed CR spectrum as in Equation (5). The atomic hydrogen column density is  $2.1 \times 10^{22} \text{ cm}^{-2}$  and  $8.0 \times 10^{22} \text{ cm}^{-2}$  for the molecular hydrogen.

of the total contribution from atomic and molecular hydrogen. The emission beyond 3 kpc arises predominantly (80%) from the more uniformly distributed HI gas.

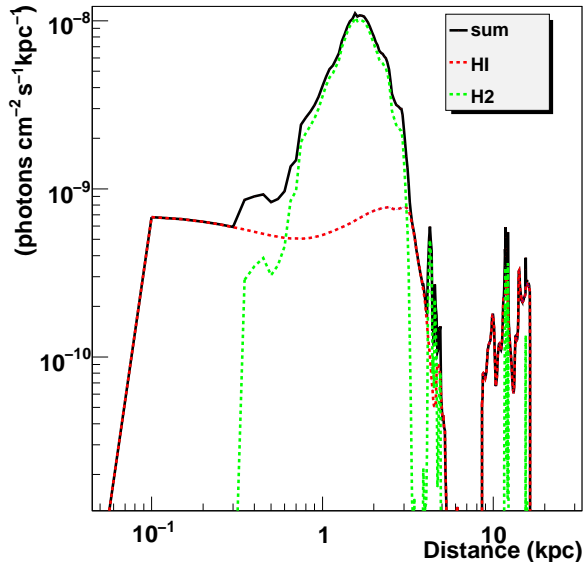
The Fermi Collaboration quotes an integral sensitivity of  $5 \times 10^{-10} \text{ photons cm}^{-2} \text{ s}^{-1}$  above 1 GeV from a region which has an angular resolution of 0.7 by 0.7 degrees. This makes the detection of the predicted emission for Fermi possible. Future Cherenkov telescopes, such as CTA, will need to reach a sensitivity of about  $5 \times 10^{-12} \text{ photons cm}^{-2} \text{ s}^{-1}$  for observing a region of 0.7 by 0.7 degrees above 100 GeV.

We have here presented a methodology to test the cosmic ray flux in discrete distant regions of the Galaxy by combining the most recent high resolution  $\gamma$ -ray and gas data. By assuming a flat rotation curve model of the Galaxy we have estimated the gas number density at discrete positions as a function of the heliocentric latitude, longitude and distance. Through the knowledge of the gas number density we have determined the total mass of the gas in discrete regions of the Galaxy and there we have predicted the  $\gamma$ -ray emissivity under the assumption that the CR flux is equal to that measured at Earth. By comparing the predicted and the measured  $\gamma$ -ray flux we have obtained a test of the level of the CR flux in these regions. The CR flux has been calculated as a function of the Galactic longitude, latitude and heliocentric distance, providing a sort of *tomography* of the CR flux in different locations of the Galaxy.

For our investigations we have used the higher resolution  $^{12}\text{CO}$  (viz. 4' NANTEN data) and LAB HI surveys. The resolution of the LAB HI data used in the

**Table 1.** Summary of parameters as a function of distance for the region  $345.3^\circ < l < 346^\circ$  and  $1^\circ < b < 1.7^\circ$ 

| Region<br>(kpc) | Mass<br>( $M_\odot$ ) | Mass (H <sub>2</sub> )<br>( $M_\odot$ ) | Mass (HI)<br>( $M_\odot$ ) | F( E > 1 GeV)<br>( $\text{cm}^{-2} \text{s}^{-1}$ ) | F(E > 100 GeV)<br>( $\text{cm}^{-2} \text{s}^{-1}$ ) |
|-----------------|-----------------------|---|----------------------------|---|--|
| (1)             | (2)                   | (3)                                     | (4)                        | (5)   | (6)  |
| $0.5 < d < 30$  | 20.2                  | 4.2                                     | 16.0                       | $1.7 \times 10^{-8}$                                | $6.8 \times 10^{-12}$                                |
| $d < 0.5$       | 0.0015                | 0.0005                                  | 0.001                      | $2.9 \times 10^{-10}$                               | $1.2 \times 10^{-13}$                                |
| $0.5 < d < 3$   | 3.2                   | 2.8                                     | 0.4                        | $1.4 \times 10^{-8}$                                | $5.7 \times 10^{-12}$                                |
| $d > 3$         | 17.0                  | 1.4                                     | 15.6                       | $2.3 \times 10^{-9}$                                | $9.1 \times 10^{-13}$                                |

**Fig. 7.** Flux above 1 GeV as function of the line of sight distance in units of  $\text{cm}^{-2} \text{s}^{-1} \text{kpc}^{-1}$ , produced by CRs interacting with the atomic and molecular gas. The atomic hydrogen is uniformly distributed in the Galactic Plane, whereas the molecular hydrogen is more localised.

present investigation is 0.6 deg. The high resolution of the NANTEN data allows for the first time detailed comparisons of our  $\gamma$ -ray predictions with new TeV and multi-GeV data. In future we will make use of the higher resolution (2 arcmin) Southern Galactic Plane HI Survey available at <sup>3</sup>, in order for our predictions to match with higher resolution TeV data in cases where the  $\gamma$ -ray component from HI is similar to or dominates over the  $\gamma$ -ray component from H<sub>2</sub> (e.g from Figure 4 in the 10 to 15 kpc range).

#### 4.1. Uncertainties in the CR flux estimate

Uncertainties in the distance estimates affect the calculation of the CR flux in Equation (2) in three ways. Firstly, in the determination of the conversion factor  $X$  in Equation (1), by which the emissivity of the CO line is converted to ambient matter density. As previously discussed, the uncertainty in the  $X$  factor is 50% (Arimoto et al. 1996). Secondly, there are uncertainties in the de-

termination of the number density of H<sub>2</sub> molecules from the measured CO intensity. Specifically, the error on the distance (especially at small distances; c.f. Fig.1) is as large as 2 kpc. We note however, that for extended sources (i.e., sources whose intrinsic size is larger than the beam size), Equation (2) shows that the CR flux density is proportional to the distance squared and inversely proportional to the mass. Since the mass scales as the distance square, the relative errors exactly cancel. For unresolved sources (i.e., sources whose intrinsic size is smaller than the beam size), we note that the above errors still hold, however, there will be a systematic underestimation of the true CR flux density because of beam dilution. Thus estimates for the CR flux density need to be estimated using *extended* sources only.

It is instructive to note that only 85% of the emission, which would be measured from the direction  $345.3^\circ < l < 346^\circ$  and  $1^\circ < b < 1.7^\circ$ , is produced in the region  $0.5 \text{kpc} < d < 3 \text{kpc}$ . Therefore only this 85 % of the emission is to enter in Equation (2) in order to estimate the CR flux in the region  $0.5 \text{kpc} < d < 3 \text{kpc}$ . Moreover, part of the  $\gamma$ -ray emission, which would be measured from the region  $345.3^\circ < l < 346^\circ$  and  $1^\circ < b < 1.7^\circ$ , is produced through competing IC and non-thermal bremsstrahlung mechanisms of primary and secondary electrons. In particular, in the energy range between 10 MeV and 100 MeV bremsstrahlung processes of background and secondary electrons produce a non negligible contribution to the  $\gamma$ -ray emission, so that the presented method can be applied to the analysis of the  $\gamma$ -ray emission above 100 MeV-1 GeV, where moreover the angular resolution of the Fermi LAT detector is substantially better. Finally unknown CR source(s) might produce an enhancement of the local CR background.

## 5. Conclusions

The CR level in distant regions of the Galaxy and the distribution of Galactic CR sources are unknown.  $\gamma$ -rays emitted when CR protons and nuclei interact with the atomic and molecular gas have been long recognised as a unique probe of the CR flux and spectrum in the Galaxy (Ginzburg & Syrovatskii 1964 ; Puget & Stecker 1974 ; Casse & Cesarsky 1976 ; Bloemen et al 1984 ; Bloemen et al 1986 ; Lebrun et al. 1982 ; Bertsch et al. 1993 ; Strong et al. 2004 ).

We have here introduced a methodology which aims to provide a test bed for current and future  $\gamma$ -ray observato-

<sup>3</sup> <http://www.atnf.csiro.au/research/HI/sgps/queryForm.html>



ries to explore the cosmic ray flux at various positions in our Galaxy. In order to investigate the CR spectrum in distant regions of the Galaxy we have here assumed that the CR flux and spectrum measured at the Earth is representative of the typical CR flux and spectrum present throughout the Galaxy. The  $\gamma$ -ray emission arising from such CR spectrum has been calculated in specific regions of the Galaxy, using the knowledge on the distribution of the atomic and molecular gas, as given by the LAB and Nanten surveys, respectively. The peaks in the longitudinal and latitudinal distributions of the gas correspond to directions in the Galaxy, where only one or at most few massive clouds contribute to the total mass. This can be demonstrated by studying how the gas is distributed along the line of sight distance. We have then exploited this knowledge of the gas number density point by point to determine the total mass of the gas of some MCs of the Galaxy. From the total mass of the atomic and molecular gas we have calculated the level of the  $\gamma$ -ray emission in such gas clouds. The predicted  $\gamma$ -ray emission from such gas clouds can be compared with observations of present and future  $\gamma$ -ray detectors and provide a test of the CR density in distant locations of the Galaxy. We have, in particular, demonstrated that the new high quality data of NANTEN and the performance of the Fermi LAT telescope are sufficient for meaningful probes of CR densities in specific localised regions.

Equation (2) shows that the CR flux density is proportional to the distance squared and to the  $\gamma$ -ray ray flux and inversely proportional to the mass of the MC. The error in the determination of distances (especially at small distances; c.f. Fig.1) is as large as 2 kpc. We note however, that for extended sources (i.e., sources whose intrinsic size is larger than the beam size) the mass scales as the distance square and the relative errors on mass and distance exactly cancel. Moreover, above 100 MeV - 1 GeV, the competing leptonic processes, bremsstrahlung and IC of background and secondary electrons, produce a negligible contribution to the  $\gamma$ -ray emission. The emission from molecular clouds, located far from strong CR sources, is then the footprint of the CR *sea* within the cloud and molecular clouds serve then as *barometers* of the CR pressure. The detection of even a single under-luminous cloud with respect to the predictions based on the local CR density would cast severe doubt on the assumption that the level of the observed CR flux is representative of the average CR flux and spectrum in the Galaxy. This conclusion is even reinforced if additional gas, not yet revealed, is present in the cloud. In this regard, by comparing various interstellar gas tracers, EGRET  $\gamma$ -ray sky maps, HI and CO lines but also dust thermal emission, Grenier et al. 2005 unveiled clouds of dark gas surrounding the nearby CO clouds. Grenier et al. 2005 concluded that the additional mass from dark clouds implies that the cosmic ray densities are overestimated in regions rich in dark clouds.

A detailed analysis of the spectral features of the  $\gamma$ -ray emission from various regions of the Galaxy is also crucial. In fact, deviations from the standard spectrum are indications of local CR sources. The regions in the

Galaxy where the spectral features and/or the normalisation of the  $\gamma$ -ray spectrum cannot be explained by interactions of a CR spectrum similar to that measured close to the Sun, are of interest to probe the sites of Galactic CR injection, such as SNRs and pulsars.

The Fermi observatory, which detects  $\gamma$ -rays in the energy range between tens of MeVs and hundreds of GeVs and which benefits by a large effective area and good angular resolution, is an ideal instrument to perform survey of extended diffuse sources such as molecular clouds in the Galaxy. Additionally, future VHE detectors, such as CTA, will offer improved sensitivity and angular resolution, close to the angular resolution of the NANTEN survey, and could investigate the morphology of the  $\gamma$ -ray emission and compare it to the structures of molecular hydrogen clouds in the Galaxy. Future IACT telescopes ability to resolve clouds will of course strongly depend upon the instrument sensitivity to detect extended sources. On the other hand, future large field of view experiments, such as HAWC, will be able to investigate the level of the cosmic ray background on large portions of the sky (Aharonian, Buckley, Kifune & Sinnis 2008 ).

Finally, we note that we have applied our analysis of the spectral line observations to predict the  $\gamma$ -ray emission in only one distant region. It serves mostly as a 'proof-of-concept', to be followed by a more comprehensive study of the entire Galaxy.

## Acknowledgments

First of all we would like to thank the anonymous referee for his/her help to improve the manuscript.

The NANTEN telescope was operated based on a mutual agreement between Nagoya University and the Carnegie Institution of Washington. We also acknowledge that the operation of NANTEN was realised by contributions from many Japanese public donators and companies. This work is financially supported in part by a Grant-in-Aid for Scientific Research from the Ministry of Education, Culture, Sports, Science and Technology of Japan (Nos. 15071203 and 18026004, and core-to-core program No. 17004) and from JSPS (Nos. 14102003, 20244014, and 18684003).

S. Casanova and S. Gabici acknowledge the support from the European Union under Marie Curie Intra-European fellowships. We want to thank Dr Kester Smith and Joanne Dawson for very helpful discussions.

## References

- Abdo, A. A. et al, 2007, ApJL, 658, 33
- Abdo, A. A. et al, 2008, ApJ, 688, 1078
- Abdo, A. A. [Fermi Collaboration], 2009, ApJ, 703, 1249A
- Aharonian, F. A. & Atoyan, A. M., 1996, A&A, 309, 917
- Aharonian, F. A. , 2001, Space Science Reviews, 99, 187
- Aharonian, F. A. & Atoyan, A. M., 2000, A & A, 362, 937
- Aharonian, F. A. et al., 2006, Nature, 439, 695
- Aharonian, F., Buckley, J., Kifune, T. & Sinnis, G., 2008, Reports on Progress in Physics, 71, 9, pp. 096901
- Alvarez, H., May, J., & Bronfman, L. 1990, ApJ, 348, 495

- Arimoto, N., Sofue, Y. & Tsujimoto, T., 1996, PASJ, 48, 275A
- Arnal, E. M., Bajaja, E., Larrarte, J. J., Morras, R., Pöppel, W. G. L., 2000, A & A Supplement, 142, 35-40
- Atoyan, A. M. & Aharonian, F. A., 1996, A&AS, 120, 453
- Bertsch, D. L. et al., 1993, ApJ, 416, 587
- Berezinskii, V. S., Bulanov, S. V., Dogiel, V. A. & Ptuskin, V. S., Astrophysics of Cosmic Rays, Amsterdam: North-Holland, 1990, edited by Ginzburg, V.L.
- Bloemen, J. B. G. M., Caraveo, P.A., Hermsen, W. et al., 1984, A&A 139, 37
- Bloemen, J. B. G. M. et al., 1986, A&A, 154, 25
- Paul, J., Casse, M. & Cesarsky, C. J., 1976, ApJ, 207, 62P
- Clemens, D. P. 1985, Apj, 295, 422
- Dermer, C., 1986, A&A, 157, 223
- Duncan, A.R., Stewart, R.T., Haynes, R.F., et al, 1995, MNRAS, 277, 36
- Fukui, Y. et al., 1999, PASJ, 51, 6
- Fukui, Y. et al., 2001, PASJ, 53, 6
- Fukui, Y. et al., 2008, e-Print: arXiv:0810.5416
- Gabici, S., Aharonian, F. A., & Blasi, P., 2007, Astrophysics and Space Science, 309, 1-4, 365-371
- Gabici, S. & Aharonian, F. A., 2007, ApJL, 665, 131
- Gabici, S. et al., 2008, Astroparticle Physics, 30, 167
- Gabici, S., Aharonian, F. A., & Casanova, S., 2009, Monthly Notices of the Royal Astronomical Society, 396, 1629
- Ginzburg, V. L. & Syrovatskii, S. I., 1964, The Origin of Cosmic Rays, Pergamon Press
- Grenier, I. A., Casandjian, J., & Terrier, R., S., 2005, Science, 307, 1292
- Hartmann Dap & Burton, W. Butler, 1997, Atlas of Galactic Neutral Hydrogen, by Dap Hartmann & W. Butler Burton, pp. 243. ISBN 0521471117. Cambridge, UK: Cambridge University Press
- S. D. Hunter et al., 1997, ApJ, 481, 205H
- Indriolo, Nick, Geballe, Thomas R., Oka, Takeshi, McCall, Benjamin J., 2007, Apj, 671, 1736I
- Indriolo, Nick, Fields, Brian D., McCall, Benjamin J., 2009, Apj, 694, 257
- M. R. Issa and A. W. Wolfendale, 1981, Nature, 292, 5, 430-433
- Jones, D. I., Crocker, R. M., & Protheroe, R. J., 2008, PASA, 25, 161
- Jones, D. I., Crocker, R. M., Ott, J., et al., AJ submitted
- Kalberla, P.M.W., Burton, W.B., Hartmann, Dap, Arnal, E.M., Bajaja, E., Morras, R., & Pöppel, W.G.L. (2005), AA, 440, 775
- Kelner, S. R., Aharonian, F. A. & Bugayov, V. V., 2006, Phys ReV D 74, 034018
- Lebrun, F., Paul, J. A., Bignami, G. F., Caraveo, P. A., Buccheri, R., Hermsen, W., Kanbach, G., Mayer-Hasselwander, H. A., Strong, A. W. & Wills, R. D., 1982, A&A, 107, 390-396
- Strong, Andrew W. & Moskalenko, Igor V., 1998, ApJ, 509, 212S
- Mizuno, A. & Fukui, Y. 2004, ASP Conf. Proc., 317, 59
- Mori, M., 1997, Apj, 478, 225
- Nakanishi, H. & Sofue, Y., 2003, PASJ, 55, 191
- Nakanishi, H. & Sofue, Y., 2006, PASJ, 58, 847
- Particle Data Group, 2008, Phys. Lett. B, 667, 212
- Protheroe, R. J., Ott, J., Ekers, R. D., et al., 2008, MNRAS, 390, 683
- Puget, J. L. & Stecker, F. W., 1974, ApJ, 191, 323P
- Strong, A. W., Moskalenko, I. V. & Reimer, O., 2004, ApJ, 613, 962